Wind Engineering Joint Usage/Research Center
FY2018 Research Result Report

Research Field: Wind disaster and wind resistant design
Research Year: FY2018
Research Number: 162003
Research Theme: Aerodynamic coupling of wind-exited tall buildings with structural connections

Representative Researcher: Prof. Tim K.T. Tse

Budget [FY2018]: 330,000Yen

*There is no limitation of the number of pages of this report.
*Figures can be included to the report and they can also be colored.
*Submitted reports will be uploaded to the JURC Homepage.

1. Research Aim

This study investigated the aerodynamic characteristics of two tall buildings through an independent component analysis (ICA) and principal component analysis (PCA) of wind-induced pressure fields. Furthermore, this study presents the optimal location and properties (e.g., mass and stiffness) of a structural link for a linked building (LB) system. The objective of this study is to minimize not only the wind-induced displacement responses but also the wind-induced acceleration responses of the LB systems.

2. Research Method

The two prototype buildings used in this study were 160 m tall with a floor plan measuring 30 × 30 m. For the wind tunnel experiment, building models were fabricated at 1/300 scale. The wind tunnel tests were conducted in the boundary layer wind tunnel of the CLP Power Wind/Wave Tunnel Facility at Shimizu Corporation, Japan. The dimensions of the wind tunnel are 3.5 m (W) × 2.5 m (H). To examine the effects of the gap between buildings, the interference effects were considered to be functions of this distance. Thus, five cases were investigated with the two tall buildings separated by different gaps. A synchronous multi-pressure measurement system (SMPMS) was used to measure wind pressure fluctuations on the surfaces of the two buildings. The calibration and the measurement tasks were fully computer controlled. The measured pressures on all the building surfaces were expressed as a pressure coefficient relative to the reference pressure. The reference pressure was measured slightly above the top of the building model. In the present study, to investigate the basic aerodynamic characteristics of the building group, the instantaneous wind flows around the two buildings were measured via PIV, conducted at the same elevation as the SMPMS, i.e., 0.8 H. Measurements were taken in the horizontal plane around the two buildings at this elevation as well. The sample frequency for the PIV was 150 Hz, and the SMPMS and PIV were synchronized during the wind tunnel tests. Figure 1 depict the setup for the PIV and SMPMS tests.

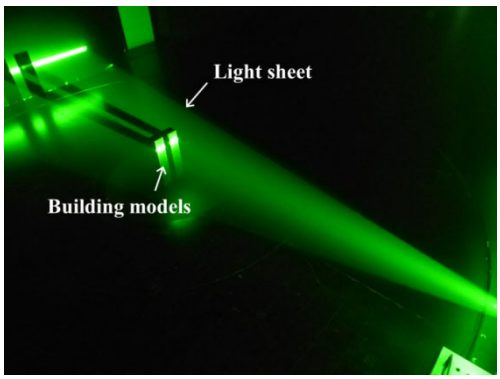

Fig. 1. Test model and experimental setup

For optimum design, this study uses an illustrative example of an LB system. Structural components, structural properties, and the prototype dimensions of the two buildings of the considered LB system are the same. However, the structural link's properties, gap distances and location vary in this analytical model. Figure 2 represents an example of an LB system connected by a structural member on the top of the two buildings. The prototype of two buildings of the LB system is 160 m in height with a floor plan of 30 m × 30 m, which is typical of an LB system. Each building has a frame-core wall structure. Such a structure was used for an LB system in past studies to formulate an analytical model. In this study, an optimization method for the formulated analytical model was introduced to minimize the wind-induced responses and to create an optimal structural design for the structural link.

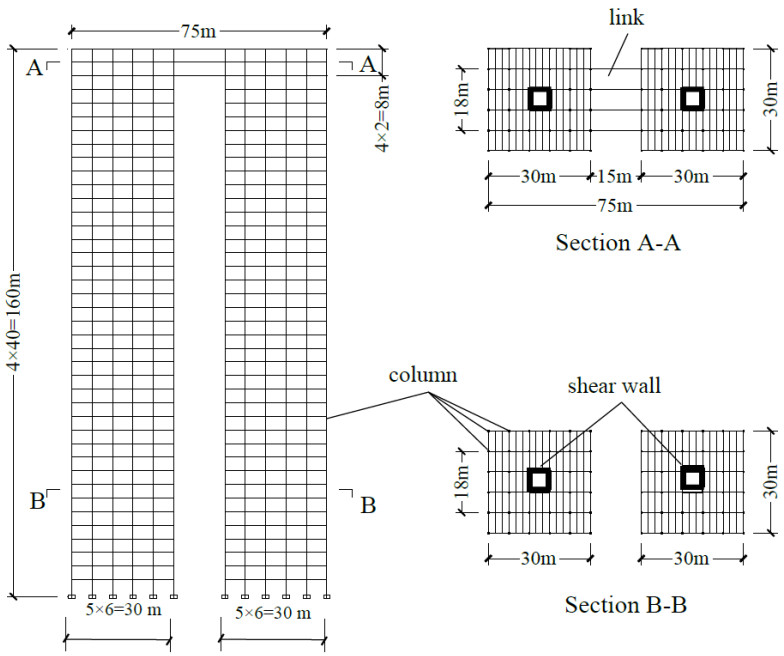

Fig. 2. Structural system of an LB system

Wind force components were measured to calculate the wind-induced lateral responses of the LB system. In a series of wind tunnel tests, a synchronous multi-pressure measurement system (SMPMS) was applied to obtain pressure coefficients on the all surfaces of the two building models. The effect of the link is local, because the link is relatively small and not important effect on the global wind forces. For this reason, LB systems with different properties of the structural link are then supposed to be subjected to the same wind loads, regardless of link location, as shown in Figure 3.

An SMPMS with nine levels of taps on each surface and five taps on each level was installed. As a result, the total number of pressure taps of the LB system was 360, measuring the wind pressure coefficients on each surface. With the measured wind pressure data at each pressure tap installed on the each surface of the LB model, the along-wind, cross-wind, and torsional wind forces of the two buildings of the LB systems can be investigated.

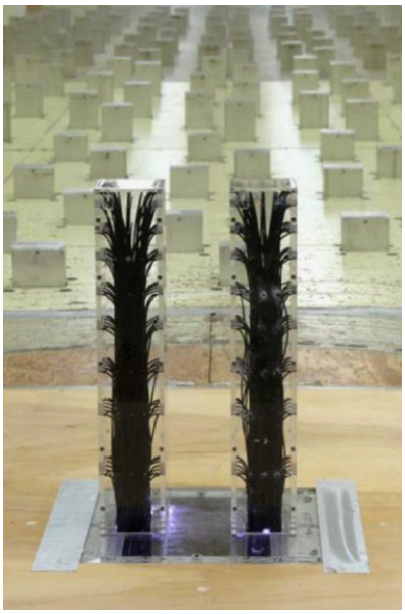

Fig. 3. Two building models in the wind tunnel

3. Research Result

When the gap is small, the two buildings behave as a single bluff-body, because vortex shedding occurs mainly in the outer shear layers. Occasionally, a weak wind flow in the gap between the two buildings was observed. In the present study, we define the inner shear layer as that shear layer generated between the two buildings, and the outer shear layer as the shear layer generated in locations other than between the two buildings. As shown in Figure 4, an inherently biased flow is observed in the space between the two buildings for this small gap, while an oscillating asymmetric flow pattern is observed between the two buildings. Because of the biased flow in this gap area, the pressure patterns on the side surfaces of the two buildings take different forms to those that appear on the other surfaces. Further investigation of these pressure patterns is necessary in ICA and PCA, as described in the next part.

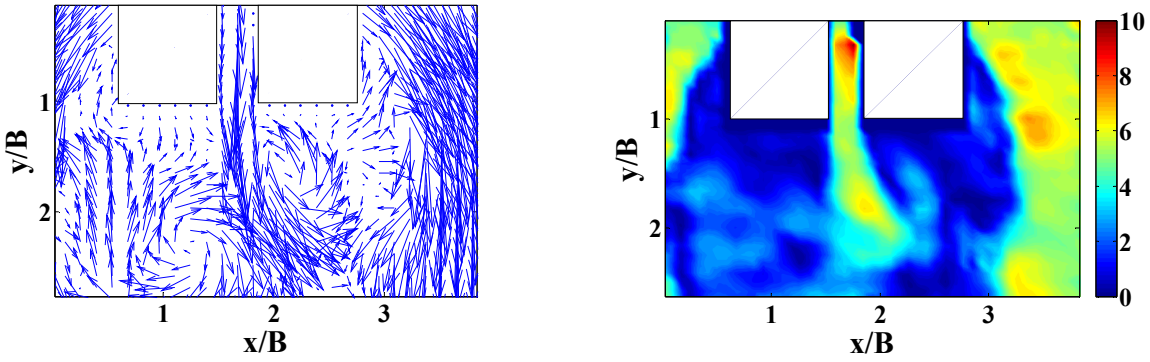

(a) Instantaneous velocity vectors (b) Instantaneous velocity (m/s)

Fig. 4. Flow pattern with smallest gap

Though PIV directly provides flow visualization information, the wind flow patterns around the two buildings can be only used to assess instantaneous aerodynamic characteristics. The use of ICA allows the pressure pattern characteristics to be investigated over the entire measurement time. Accordingly, this section discusses the pressure pattern results obtained via ICA.

When using PCA for the side-by-side buildings, the energy contribution was highest in the 1st mode, while the energy contribution tended to decrease as the mode increased. Because the pressure patterns resulting from all modes cannot be discussed in detail due to length limitations, this paper focuses on the first four modes, as they are relatively more important.

In the investigation of the instantaneous wind flows and the mean wind velocity around the two buildings presented, the shear layers that arose between the two buildings interacted with each other and a variety of pressure patterns on the inside surfaces were predicted. However, it was not possible to investigate the overall aerodynamic characteristics arising between the two buildings during the measurement period using instantaneous wind flows alone. Accordingly, an additional statistical analysis such as ICA is required.

The 1st, 2nd, and 4th modes shown in Figure 5 displayed notable variations in pressure patterns on the inside and windward surfaces, according to the gap, compared to the other surfaces. As shown in Figure 5 (a), because the suction force on the inside surface is high, the negative pressure on the inside surfaces near the windward edges of the two buildings is relatively large. However, this negative pressure decreases as the gap increases. According to Figure 5 (b), the 2nd mode features high pressure on the windward surface, with the inside surface pressure increased by the channeling effect. The suction effect on the inside surface becomes more apparent as the gap decreases. Additionally, as shown in the 4th mode in Figure 5 (d), the gap also affects the windward surface. In general, the pressure distributions on the windward surfaces are asymmetrical due to the channeling effect. However, this channeling effect decreases as the gap increases because, if the gap is sufficiently large (S/B = 1.5), a symmetrical pressure pattern arises on the windward surface, and a relatively large negative pressure occurs on the inside surface.

It appears that the inside surface pressure distribution in the 1st, 2nd, and 4th modes changes due to the channeling effect between the two buildings. All the pressure patterns collected by ICA can aid in understanding the development of pressure distributions on the two buildings. On the other hand, the 3rd mode in Figure 5 (c) exhibits a pressure pattern on the outside and leeward surfaces that is unaffected by the channeling effect. Therefore, only the suction effect caused by the wake flow is observed, and the pressure distribution on the outside and leeward surfaces does not change with the gap because the channeling effect is relatively weak.

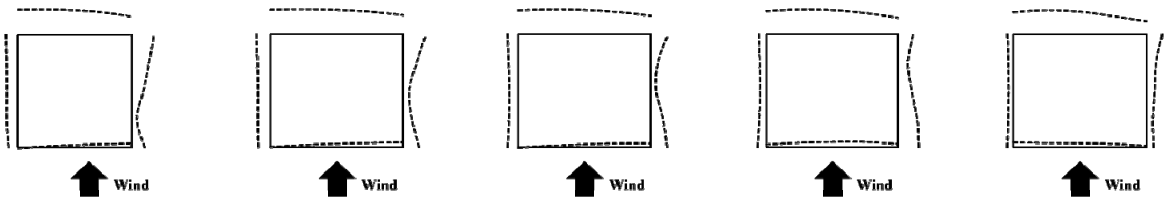

S/B = 0.33 S/B = 0.5 S/B = 0.67 S/B = 1 S/B = 1.5

(a) 1st mode

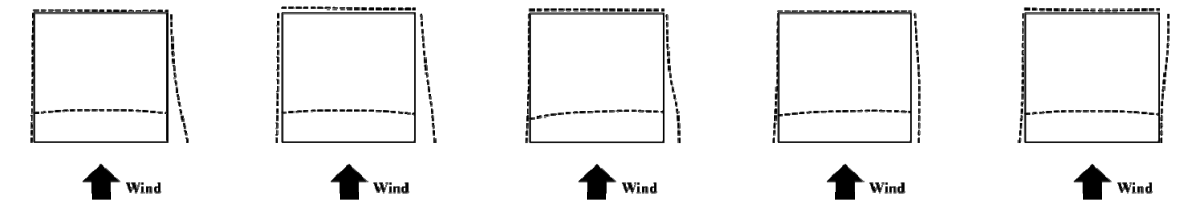

(b) 2nd mode

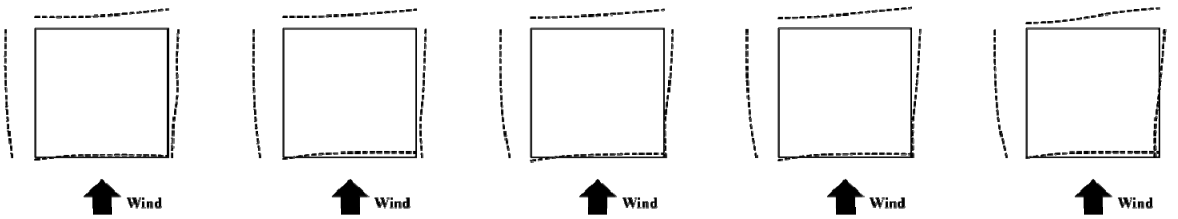

(c) 3rd mode

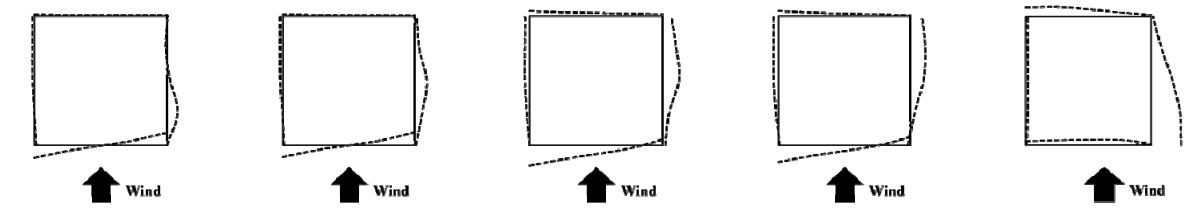

(d) 4th mode

Fig. 5. Modes of ICA

For comparison with the ICA results, the PCA results are briefly summarized in this section. All the PCA modes in Figure 6 exhibit similar low-pressure magnitudes and distributions on the outside and leeward surfaces, regardless of the gap. However, the pressure patterns on the inside surfaces clearly vary with the gap due to the channeling effect between the two buildings. The gap between the two buildings obviously plays an important role in determining the pressure magnitude on these inside surfaces.

When the gap is small (e.g., S/B = 0.33), the gradient of the pressure distribution on the inside surfaces is high because the channeling effect increases the suction force on the two inside surfaces. However, when the gap is larger (e.g., S/B = 1.5), the channeling effect becomes relatively weak and the suction force decreases, producing a smaller pressure distribution gradient on the inside surface, as shown in the 1st and 2nd modes.

When the pressure distribution on the inside surface is very strong, the gap flow is strong between the two buildings. In addition, the shear layers from the two inner edges roll up into the rear region of the two buildings through the gap, interrupting the original cross-wind correlation. As a result, various pressure patterns arise on the inside surfaces according to the gap, as shown in the 3rd and 4th modes.

Overall, the PCA results demonstrate that the tendencies of the pressure patterns on the inside surfaces are similar to those obtained using ICA, such as the channeling effect and the interaction of the shear layers of the two buildings. However, because ICA and PCA are based on different formulations, it is well known that each analysis provides different insights into the pressure patterns, with PCA concentrating on explaining the diagonal elements and ICA related to the off-diagonal elements of the covariance matrix.

In the present study, a comparison of ICA and PCA modes has demonstrated that ICA is

able to identify the characteristics of the pressure distribution on each surface as a function of the gap in each mode. In the 1st, 2nd, and 4th modes, the pressure distributions on the windward and side surfaces were shown to be function of gap, while in the 3rd mode, similar pressure patterns were shown regardless of the gap. On the outside and leeward surfaces, a high negative pressure was observed due to the influence of the wake flow. Therefore, the 3rd mode exhibits the pressure patterns of the outside and leeward surfaces, which are far less influenced by the gap than the inside and windward surfaces.

On the other hand, PCA mostly identifies variations in the pressure distribution on the inside surfaces with the change in gap between the two buildings. On the other surfaces, high positive or high negative pressure patterns did not occur. The pressure pattern variations with the gap were similar, and thus it was difficult to identify the influence of the gap.

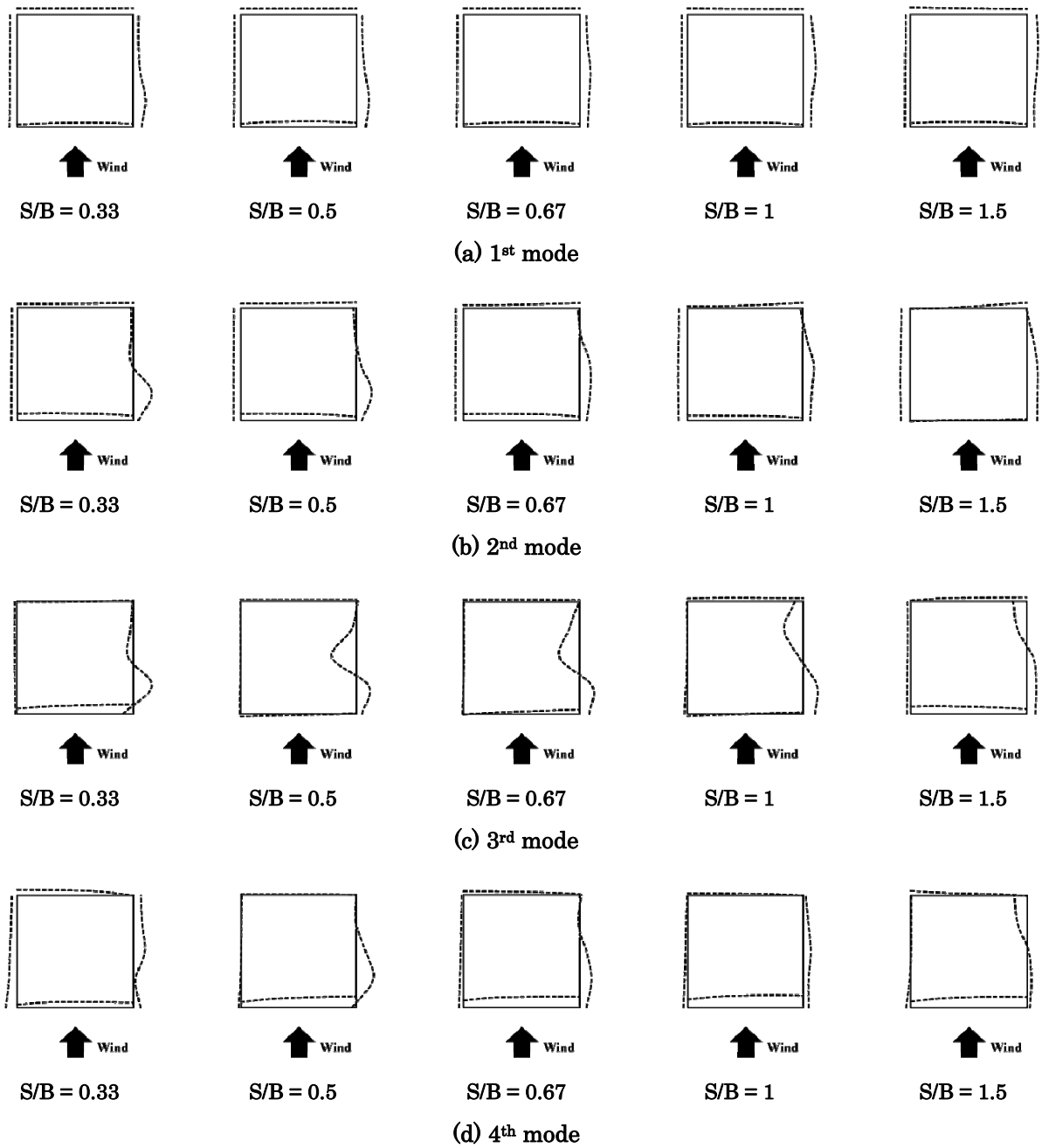

Fig. 6. Modes of PCA

The trajectories provided by ICA and PCA were used to investigate the correlations between the along-wind forces and the cross-wind forces. There is a positive correlation for S/B = 0.33, as shown in Figure 7. (In this study, a positive correlation means that when the along-wind forces increase, the cross-wind forces also increase, and vice versa.) The pressure near the gap on the windward surfaces increases with the wind force. Furthermore, due to the effects of suction, the negative pressures on the two inside surfaces near the windward edges also increase with the wind force. Accordingly, the along-wind forces and the cross-wind forces exhibit a positive correlation for S/B = 0.33, while the trajectories of the original SMPMS data are concentrated in an inclined oval shape. The PCA results show that a positive correlation is present in the 1st mode when the gap is small, as shown in Figure 7(b); a similar trend can be observed in the 3rd mode. This means that the 1st and 3rd modes provide similar information, whereas each ICA mode yields a variety of information, as shown in Figure 7(a). In identifying pressure patterns, PCA prioritizes information related to the inside surfaces, while ICA provides information for all the surfaces. Similarly, for the aerodynamic correlation of the along-wind and cross-wind forces, PCA tended to provide important information intensively for a limited region, while ICA tended to provide a variety of information for all regions. Specifically, in Figure 7, when S/B = 0.33, the along- and cross-wind forces exhibit a positive correlation, which is important information from the original SMPMS data. In the same vein, the PCA results clearly show a positive correlation in both the 1st and 3rd modes, while the ICA results show no similar modes, thus providing a wider variety of information.

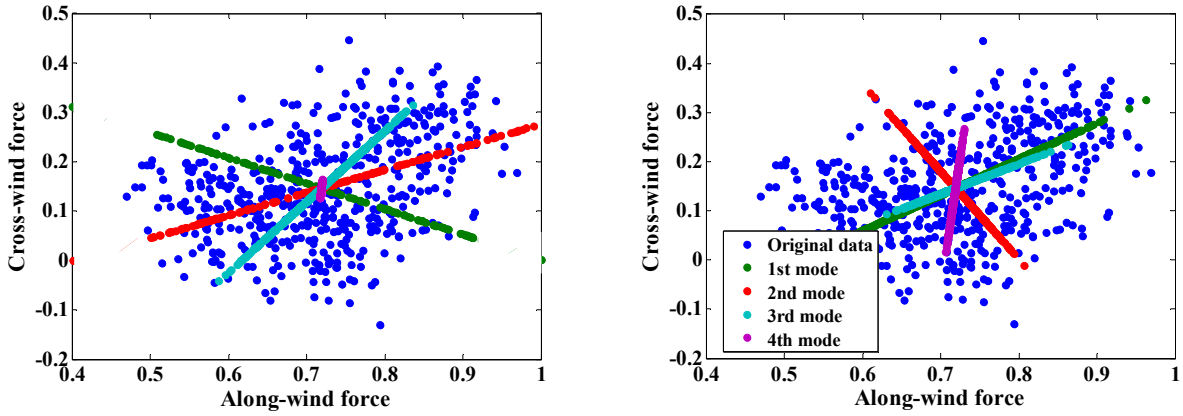

(a) ICA (b) PCA

Fig. 7. Aerodynamic correlation

For optimum design, the effects of gap ratio are complicated. Along-wind force components are insensitive to the gap ratio, but cross-wind force components are very sensitive to it. The cross-wind forces for S/B = 0.5 and 0.33 are similar and smaller than those for S/B = 1. However, compared with S/B = 0.33, the cross-wind force components between the two buildings with S/B = 0.5 have a higher negative correlation, which is useful in reducing the wind-induced responses. As a result, the optimum gap distance is found to be S/B = 0.5 in this study as shown in Figure 8.

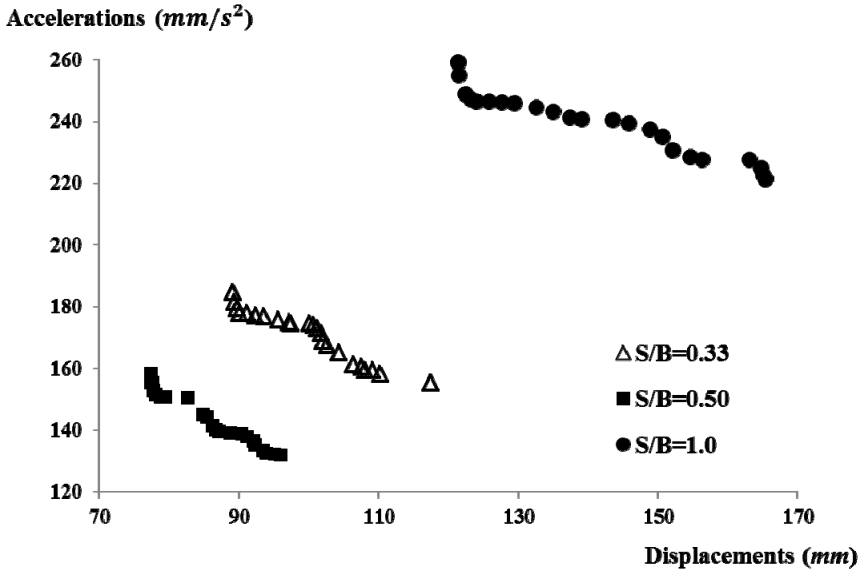

Fig. 8. Optimum solutions of all cases

4. Published Paper etc.
[Underline the representative researcher and collaborate researchers]
[Published papers]

1. Bubryur Kim, K.T. Tse, Akihito Yoshida, Yukio Tamura, Zengshun Chen, Pham Van Phuc, and Hyo Seon Park. Statistical analysis of wind-induced pressure fields and PIV measurements on two buildings, Journal of Wind Engineering & Industrial Aerodynamics, 188 (2019) 161-174.
2. Bubryur Kim, K.T. Tse, Akihito Yoshida, Yukio Tamura, Zengshun Chen, Pham Van Phuc, and Hyo Seon Park. Investigation of flow visualization around linked tall buildings with circular sections, Building and Environment, 153 (2019) 60-76.

[Presentations at academic societies]
1.
2.

[Published books]
1.
2.

[Other]
Intellectual property rights, Homepage etc.

5. Research Group
1. Representative Researcher
Prof. Tim K.T. Tse

2. Collaborate Researchers
1. Prof. Yukio Tamura
2. Prof. Akihito Yoshida
3. Dr. Hirotoshi Kikuchi

6. Abstract (half page)

Research Theme
Representative Researcher (Affiliation)
Summary・Figures

The ICA results in the 1st, 2nd, and 4th modes indicated different pressure distributions on the inside building surfaces for different gaps, while the 3rd mode indicated a suction phenomenon on the outside and leeward surfaces; the PCA results indicated that the gap only influenced the pressure on the inside surfaces in the first four modes. Only the first PCA mode had a higher correlation with the original data than the ICA modes, and the ICA modes generally had higher correlations than the other modes. In wind forces, the 1st and 3rd PCA modes provided similar information, whereas all the ICA modes provided different information. Overall, ICA provided more diverse information than PCA, which yielded rather limited and homogenous information as shown in Figure A. For optimum design, the optimal gap distance should be half of the breadth of the building as shown in Figure B.

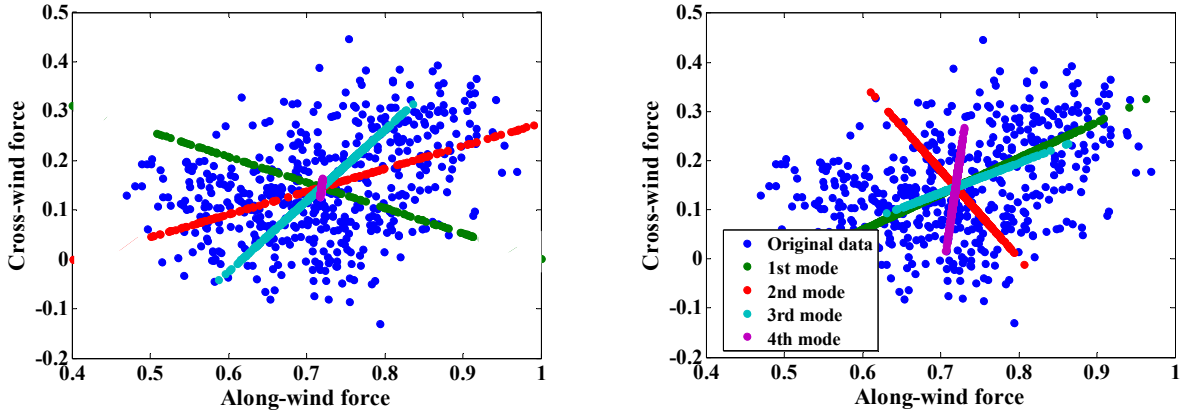

(a) ICA (b) PCA

Fig. A. Aerodynamic correlation

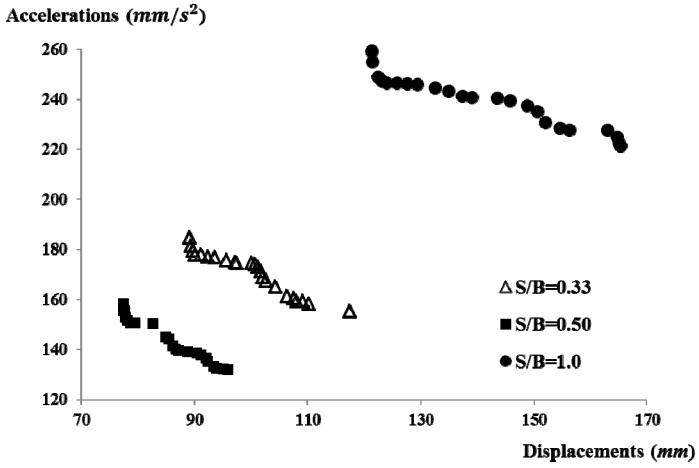

Fig. B. Optimum solutions of all cases